American Mineralogist, Volume 83, pages 1302–1315, 1998

The chemical composition of REE-Y-Th-U-rich accessory minerals in peraluminous granites of the Erzgebirge-Fichtelgebirge region, Germany. Part II: Xenotime

HANS-JÜRGEN FÖRSTER*

GeoForschungsZentrum Potsdam, Telegrafenberg, D-14473 Potsdam, Germany

ABSTRACT

Xenotime, from a geochemically heterogeneous series of mildly to strongly peraluminous granites of the Erzgebirge, Germany, displays extended compositional variability with respect to abundances of HREE, Y, U, and Th. With few exceptions, the maximum and minimum concentrations for the lanthanides and actinides exceed those noted for this mineral from other geologic environments. Xenotime chemistry is dominated by the theoretical end-members HREE-PO_4 and YPO_4 (>90 mol% in total). Typical xenotime grains from the Erzgebirge granites and from other granites worldwide contain 70–80 mol% YPO_4, and 16–25 mol% HREE-PO_4. This study documents the occurrence of xenotime, abnormally rich in HREE in place of Y, with up to 45 mol% HREE-PO_4. Substitutions of thorite-coffinite, (Th,U,Pb)SiO_4, brabantite, (Ca,Th,U)$(PO_4)_2$, and monazite, (La-Sm)PO_4, are of minor importance, reaching maximum levels of 5–6 mol% each with a total contribution typically $\ll$10 mol%. Typically, the incorporation of actinides in xenotime from these and other granites, as well as from other rocks, is dominated by thorite-coffinite substitutions. However, in some xenotime grains, the U and Th concentrations are largely accounted for by the substitution mechanism 2 $(REE,Y)^{3+} \leftrightarrow (Th,U)^{4+} + Ca^{2+}$. The total lanthanide and actinide contents in xenotime and host granite are not strongly correlated. However, formation of xenotime unusually rich in HREE occurs only in the A-type Li-mica granites that are strongly enriched in these elements. The shapes of HREE patterns of xenotime and host rock are similar which, combined with mass-balance calculations, indicate the importance of this mineral in affecting the HREE as well as Y evolution of late-stage granitic melts. Late xenotime may show strong Y/Ho fractionation, thus recording the decoupling of Y and the HREE, which can occur in the latest stages of crystallization of evolved granites and which may be associated with deuteric alteration.

INTRODUCTION

With the exception of Eu, accessory minerals constitute the major hosts of the lanthanides, yttrium, actinides, and other high field-strength elements (Zr, Hf, Nb, Ta, etc.) in various crustal rocks. Xenotime, (Y,HREE)PO_4, is an ubiquitous accessory mineral in granitic rocks of various compositions, granitic pegmatites, migmatites, and low- to high-grade metamorphic rocks. It possesses an MO_8 polyhedron that preferentially accommodates Y and the heavy rare-earth elements (HREE), owing to their smaller ionic radii compared to the light rare-earth elements (LREE), which prefer the monazite structure with an MO_9 polyhedron (Ni et al. 1995).

Xenotime is particularly abundant in Ca-poor peraluminous granites where it accounts for a large fraction of the Y and HREE (Gd-Lu) contents in bulk rocks (e.g., Wark and Miller 1993; Bea 1996a), and a significant but variable portion of the U. It typically also contains minor amounts of Th and the LREE (La-Eu), especially Nd and Sm. In xenotime-bearing peraluminous granites, the fractions of Y and total HREE contained in xenotime vary from ~30–50% (Bea 1996a).

Xenotime rarely has been studied intensively in contrast to apatite, zircon, and monazite, on which a considerable amount of experimental and analytical work has been done over the past two decades. Even many modern papers on the petrology of magmatic and metamorphic rocks overlook xenotime or simply document its presence.

The stability of xenotime in granitic melts and in their source rocks controls the distribution of Y, HREE, U, and Th between melt and restite during anatexis (Bea 1996b). Concomitant xenotime-apatite-zircon fractionation is probably responsible for the strong Y and HREE depletions commonly observed in differentiated facies of peraluminous granite plutons (Wark and Miller 1993; Förster and Tischendorf 1994). Even so, little attention has been given to the experimental study of the solubility of xenotime in granitic melts (Wolf and London 1995).

Granitic rocks may contain inherited xenotime (Miller et al. 1992), which would be useful for evaluating the age and evolution of the source material from which a silicate

* E-mail: forhj@gfz-potsdam.de

0003–004X/98/1112–1302$05.00

TABLE 1. Chemical composition of xenotime-bearing granites

	Biotite granites	Two-mica granites	S-type Li-mica granites	A-type Li-mica and biotite granites
SiO_2 (wt%)	73.5–77.1	72.3–76.6	72.4–75.7	72.0–75.1
TiO_2	0.050–0.31	0.045–0.31	0.042–0.24	0.009–0.125
P_2O_5	0.019–0.31	0.09–0.20	0.22–0.51	0.007–0.065
Y (ppm)	10.9–39.0	6.2–21.4	6.5–26.0	16.1–84.2
sum La-Sm	11.9–146	9.8–143	6.6–121	85.6–240
sum Gd-Lu	6.0–23.6	3.8–14.9	3.3–17.7	18.8–53.3
Th	4.1–39.5	4.3–18.4	3.5–20.3	8.3–51.6
U*	9.6–56.3	5.3–27.3	4.4–38.6	4.8–33.8
A/CNK	0.99–1.14	1.08–1.27	1.17–1.31	1.04–1.25

Note: A/CNK = molar $Al_2O_3/(Na_2O + K_2O + CaO)$.
* Lower values are due to post-magmatic U mobility.

magma was generated during partial melting. Despite its great potential for age dating, xenotime rarely has been used for either conventional (Köppel and Grünenfelder 1975; Hodges et al. 1992; Childe et al. 1993; Hawkins and Bowring 1997) or U-Pb measurements by ion microprobe (Kamber et al. 1996). Xenotime is one of the few minerals suited for determining Th-U-Pb mineral ages from electron-microprobe analyses (Suzuki and Adachi 1991; Rhede et al. 1996a). If cogenetic with monazite, xenotime may also serve as a geothermometer (Heinrich et al. 1997; Gratz and Heinrich 1997).

In spite of the importance of xenotime, only a few electron-microprobe studies exist on its composition. Xenotime has been analyzed from Au-bearing veins (Kerrich and King 1993), placer deposits (van Emden et al. 1997), metamorphic rocks (Suzuki and Adachi 1991; Sagon and Sabourdy 1993; Franz et al. 1996; Pan 1997), pegmatites (Åmli 1965; Demartin et al. 1991; Petersen and Gault 1993), and granitic rocks (Pointer et al. 1988; Thorpe et al. 1990; Miller et al. 1992; Ward et al. 1992; Wark and Miller 1993; Casillas et al. 1995; Förster and Rhede 1995; Bea 1996a; Förster 1997). Many of these studies, however, suffer from one or more of the following problems: (1) the host rocks exhibit only a limited range in compositional variability; (2) not enough grains were analyzed to appear fully representative; (3) the entire spec-

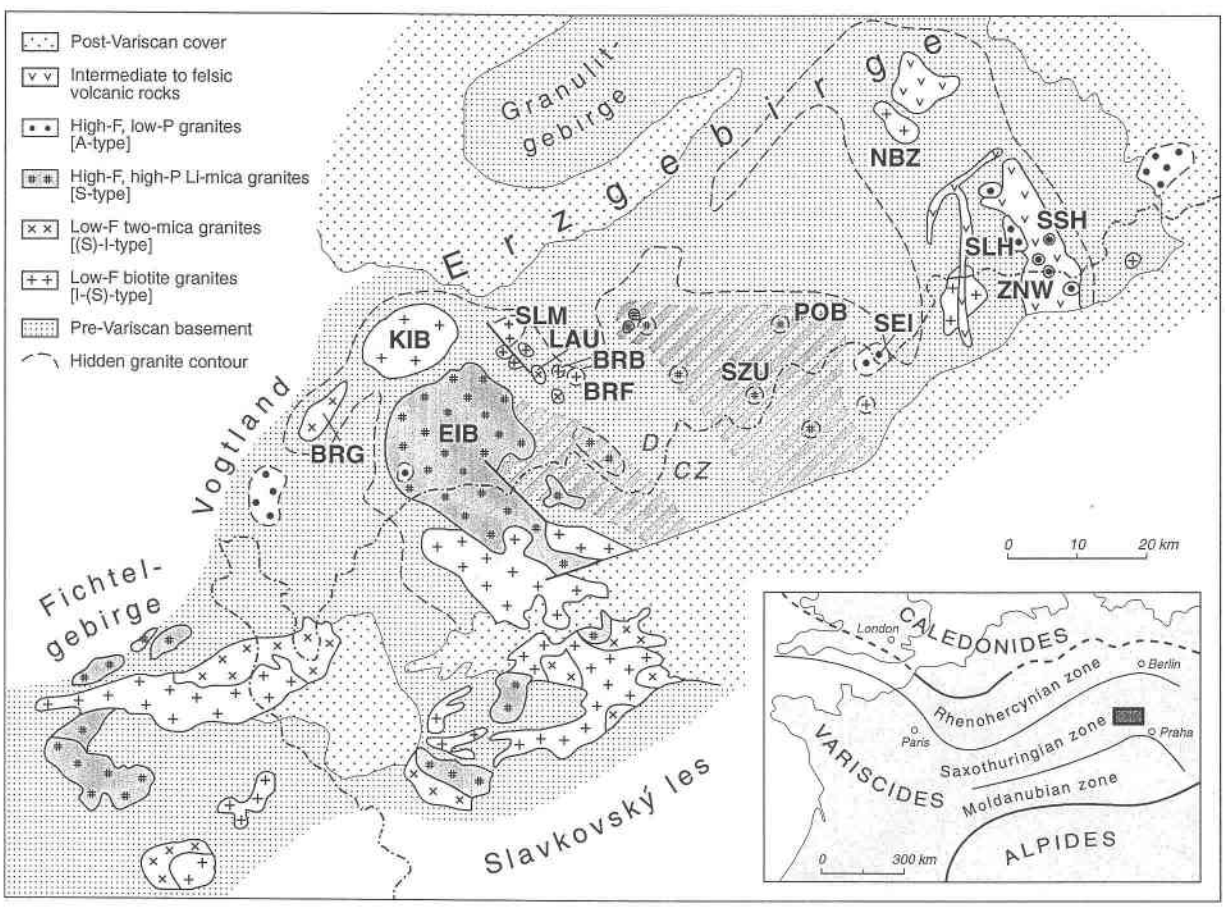

FIGURE 1. Generalized geological map of the Erzgebirge, showing the regional distribution of the different groups of Variscan granites and the plutons or intrusions from which xenotime analyses are reported in Table 2. These are (from W to E): BRG = Bergen, KIB = Kirchberg, EIB = Eibenstock, SLM = Schlema-Alberoda, LAU = Lauter, BRB = Bernsbach, BRF = Beierfeld, SZU = Satzung, POB = Pobershau, SEI = Seiffen, NBZ = Niederbobritzsch, SLH = Schellerhau, SSH = Sachsenhöhe, ZNW = Zinnwald.

TABLE 2. Electron-microprobe analyses of xenotime

	Biotite granites								Two-mica granites	
Granite	KIB	KIB	KIB	KIB	BRB	BRF	NBZ	SLM	BRG	BRG
Sample	784-F*	501-F	305-F	1073-F*	984-F*	987-F	343-F*	1000-F	823-F	478-F
Mineral host	quartz	feldspar	quartz	feldspar	feldspar	quartz	feldspar	biotite	biotite	feldspar
Analysis	1	2	3	4	5	6	7(a)	8(b)	9	10
P_2O_5	32.3	34.9	34.8	34.8	33.4	34.4	32.2	33.0	32.5	33.9
SiO_2	1.00	0.06	0.14	0.15	0.95	0.40	1.56	1.25	1.61	0.46
ThO_2	2.26	—	0.16	0.29	0.17	0.42	3.08	1.04	1.48	0.03
UO_2	5.00	0.09	—	0.32	5.51	1.14	2.66	4.29	5.78	4.49
Y_2O_3	34.8	42.2	43.9	46.1	39.6	40.4	36.0	41.0	38.5	39.2
Ce_2O_3	0.10	0.04	—	—	0.11	0.16	0.11	0.12	0.11	0.06
Pr_2O_3	0.05	0.05	—	—	0.06	0.07	0.04	0.11	0.13	0.02
Nd_2O_3	0.45	0.48	0.12	0.11	0.36	0.42	0.51	0.47	0.53	0.27
Sm_2O_3	0.73	1.28	0.25	0.10	0.34	0.67	0.71	0.44	0.45	0.10
Gd_2O_3	4.90	4.44	3.41	2.46	3.16	3.77	4.39	2.79	2.86	3.00
Tb_2O_3	1.04	0.95	0.68	0.59	0.80	0.75	0.73	0.73	0.59	0.55
Dy_2O_3	6.43	5.61	5.05	3.63	5.49	5.06	5.64	4.45	4.19	4.28
Ho_2O_3	1.31	1.28	1.26	0.91	1.14	0.89	1.10	1.00	1.01	1.10
Er_2O_3	4.35	3.59	4.01	4.10	3.99	3.59	4.02	3.78	4.10	3.42
Tm_2O_3‡	0.63	0.55	0.67	0.68	0.53	0.71	0.60	0.61	0.64	0.65
Yb_2O_3	4.11	3.69	4.83	4.90	3.10	5.84	3.98	4.38	4.43	5.22
Lu_2O_3	0.47	0.54	0.63	0.72	0.45	0.93	0.46	0.63	0.58	0.74
CaO	0.10	—	0.04	0.03	0.49	0.08	0.33	0.19	0.21	0.66
PbO	0.26	n.a.	n.a.	0.02	0.23	0.03	0.12	0.21	0.30	n.a.
Total	100.4	99.7	99.9	99.9	99.8	99.7	98.3	100.5	100.0	98.1
Mole fractions										
$(Th,U,Pb)SiO_4$	0.035	0.001	0.001	0.005	0.032	0.012	0.047	0.042	0.056	0.016
$(Ca,U,Th)(PO_4)_2$	0.031				0.033				0.019	0.051
$(La-Sm)PO_4$	0.017	0.022	0.004	0.002	0.011	0.016	0.017	0.014	0.015	0.006
$(Gd-Lu)PO_4$	0.262	0.218	0.206	0.164	0.203	0.232	0.235	0.198	0.217	0.207
YPO_4	0.655	0.757	0.782	0.817	0.721	0.731	0.675	0.743	0.709	0.720

Note: See Figure 1 for explanation of the abbreviations for the sampled granites. "—" indicates analyzed but not detected. n.a. = not analyzed.

* Aplites.

† Multiple analyses within zoned crystals. Xenotime intergrown with (a) = zircon and (b) = monazite. The analyses 9, 14, 20, 29, and 33 include 0.02, analysis 34 = 0.04 and analysis 32 = 0.05 wt% La_2O_3. The analyses 30 and 33 include 0.45 and 0.68 wt% F, respectively.

‡ Calculated concentrations (see text).

trum of elements potentially detectable by the method was not determined; (4) mineral analyses deviate strongly from stoichiometric compositions, even in cases for which oxide sums are close to 100%; and (5) only concentration ranges are given, which does not permit evaluation of individual analyses.

Xenotime was demonstrated to show systematic variations in composition between metapelites of different metamorphic grade (e.g., Bea and Montero 1997; Heinrich et al. 1997) and between granites and aplites within the composite S-type Sweetwater Wash two-mica granite pluton (Wark and Miller 1993). In this respect, the work by Wark and Miller is an exception among the studies on xenotime from granite. Thus, the results from this work will be compared to the observations of these authors on xenotime in the Sweetwater Wash granite.

This paper presents the results of a comprehensive electron-microprobe investigation of some 200 xenotime grains from mildly to strongly peraluminous granites (A/CNK $\approx$ 1.0 to 1.3, where A = Al_2O_3, C = CaO, N = Na_2O, and K = K_2O in moles; see Table 1) of the Variscan Erzgebirge province. Similar to a previous paper on monazite-group minerals in peraluminous granites of the region (Förster 1998a), the main goal is to document the compositional extremes of xenotime in terms of lanthanide and actinide concentrations. Results are shown separately for biotite, two-mica, S-type Li-mica, and A-type Li-mica and biotite granites. Due to the large compositional variability of their host rocks (see Table 1), this study may serve as a reference for the chemistry of xenotime from granitic rocks in general and for peraluminous granites in particular.

GEOLOGIC SETTING

In the late Carboniferous and early Permian, the Erzgebirge crust was intruded by late- to post-collisional granitic plutons of various sizes and highly variable and evolved compositions (Table 1, Fig. 1). The Erzgebirge is particularly well known for extensive development of various types of ore mineralization, with Sn and W deposits being ultimately related to the final stages of evolution of geochemically differentiated granitic melts (Štemprok and Seltmann 1994; Tischendorf and Förster 1994).

The granitic rocks are grouped into four main types based on geological, mineralogical, and geochemical criteria (Förster and Tischendorf 1994; Förster et al. 1995) as listed below. Localities from which xenotime data are reported in Table 2 are given in parentheses and are shown in Figure 1. The ranges in composition and A/

TABLE 2—*Continued*

Two-mica granites			S-type Li-mica granites							
BRG 1085-F biotite 11	LAU 807-F feldspar 12	LAU 807-F quartz 13	EIB 504-F biotite 14	EIB 820-F feldspar 15	EIB 509-F Li-mica 16(a)	EIB 320-F Li-mica 17	EIB 1065-F feldspar 18	SZU 926-F biotite 19	SZU 934-F Li-mica 20(a)	POB 911-F Li-mica 21
34.2	34.1	32.7	32.3	34.3	34.6	33.4	33.4	34.2	34.0	33.8
0.49	0.42	1.51	1.60	0.48	0.30	1.11	0.94	0.56	0.68	0.85
0.51	0.57	1.58	1.42	0.25	0.57	1.23	1.09	0.77	0.71	1.21
2.09	1.85	4.71	6.41	3.69	2.86	3.52	4.31	3.28	4.36	3.18
42.0	40.9	39.2	39.2	39.7	43.2	40.4	39.7	42.2	39.6	42.2
0.05	0.08	0.12	0.20	0.11	0.08	0.16	0.11	0.04	0.11	0.23
0.02	0.04	0.07	0.05	0.06	0.02	0.08	0.05	—	0.05	0.08
0.51	0.25	0.66	0.52	0.55	0.13	0.62	0.38	0.49	0.37	0.71
0.37	0.44	0.55	0.66	0.72	0.03	0.71	0.42	0.61	0.61	0.68
3.11	2.95	2.86	3.81	4.76	2.50	4.71	3.27	4.45	4.18	4.19
0.61	0.77	0.70	0.77	1.18	0.49	0.96	0.75	1.03	1.23	0.94
4.46	5.09	4.40	6.01	6.96	4.59	6.78	5.40	6.98	7.00	6.63
0.99	1.00	1.04	1.15	1.19	1.21	1.02	0.97	0.98	0.97	1.07
4.04	3.57	3.69	2.49	2.57	3.54	1.99	3.52	2.28	2.52	2.39
0.70	0.74	0.63	0.30	0.34	0.52	0.21	0.54	0.27	0.35	0.25
5.23	6.30	4.63	1.48	1.92	3.43	0.73	3.63	1.00	2.11	0.92
0.70	0.94	0.68	0.26	0.28	0.46	0.11	0.55	0.18	0.39	0.15
0.12	0.16	0.15	0.43	0.50	0.55	0.64	0.60	0.44	0.55	0.33
0.08	0.09	0.22	n.a.	0.16	n.a.	n.a.	0.16	0.13	0.20	0.13
100.3	100.3	100.0	99.1	99.7	99.1	98.4	99.8	100.0	99.9	99.9
0.017	0.014	0.051	0.055	0.016	0.010	0.036	0.032	0.019	0.023	0.029
	0.007		0.024	0.038	0.032		0.032	0.024	0.041	0.012
0.011	0.100	0.017	0.018	0.017	0.003	0.019	0.011	0.014	0.014	0.020
0.223	0.229	0.203	0.181	0.210	0.179	0.182	0.202	0.200	0.219	0.180
0.756	0.740	0.718	0.722	0.718	0.775	0.734	0.722	0.757	0.718	0.759

CNK ratios for those type A–D granites, in which xenotime was identified, are given in Table 2. A–D is defined: (A) biotite granites and their muscovite-bearing, aplitic differentiates (Kirchberg, Schlema-Alberoda, Beierfeld, Bernsbach, Niederbobritzsch) (B) two-mica granites with late, aplitic tourmaline-muscovite fractionates (Bergen, Lauter) (C) high-fluorine, high-phosphorus Li-mica granites (Eibenstock, Pobershau, Satzung) (D) high-fluorine, low-phosphorus biotite (Gottesberg) and Li-mica granites (Seiffen, Schellerhau, Sachsenhöhe, Zinnwald).

Groups A and B granites possess transitional I-S type affilation, with the two-mica granites (B) showing a predominance of compositional and mineralogical features characteristic of S-types (e.g., Förster and Tischendorf 1994). Group C granites are typical S-type rocks of late-collisional genesis. Group D granites, which comprise biotite- (e.g., Gottesmann et al. 1995) and Li-mica types, probably derived from different protoliths and are part of the aluminous group of post-collisional A-type igneous rocks.

ANALYTICAL METHODS

Xenotime in polished thin sections was analyzed for P, Si, Th, U, REE (except Eu and Tm), Y, Al, Fe, Ca, Pb, and F with automated CAMEBAX SX-50 and SX-100 electron microprobes at the GFZ Potsdam using wavelength-dispersive techniques. The operating conditions were as follows: accelerating voltage 20 kV, beam current 40–60 nA, and beam diameter 1–2 μm. Counting times, data reduction, analyzing crystals, standards, analytical precision, and detection limits are given in Förster (1998a). Thulium concentrations were not measured because both the $L\alpha_1$ and $L\beta_1$ lines of Tm suffer strong interferences with lines of other REE (e.g., Reed and Buckley 1998). Thus, they were interpolated from chondrite-normalized abundances of the neighboring elements Er and Yb. Eu was not measured because its concentration in natural specimens is typically much lower than 0.1 wt% (Åmli 1975; Demartin et al. 1991; Casillas et al. 1995; Bea 1996a). The concentrations of Gd were corrected empirically for interference of Gd$L\beta_1$ by Ho$L\alpha_1$ (e.g., Roeder 1985). In all analyses reported in Table 2, Al and Fe were below the detection limits (~0.03 wt%). Elements including Zr, Hf, Nb, Ta, Na, and Mg, which are occasionally reported from natural specimens in concentrations of some 100 ppm to a few thousand ppm (Petersen and Gault 1993; Casillas et al. 1995; Bea 1996a), were not sought. Backscattered-electron imaging (BSE) confirmed that individual analyses were confined to compositionally homogeneous areas.

Granite samples of approximately 2–10 kg were crushed for whole-rock analysis. Between one and three thin sections, in which the xenotime grains were studied by electron microprobe, were made from different splits of each sample. Whole-rock REE, Y, Th, and U concentrations were determined by inductively coupled plasma-

TABLE 2—*Continued*

	A-type Li-mica granites								
Granite	SEI	SEI	SEI	SEI	SLH	SLH	SSH	SSH	SSH
Sample	1056-F	1057-F	1057-F	1057-F	1141-FS	1141-FS	1173-FS	1166-FS	1166-FS
Mineral host	Li-mica	Li-mica	Li-mica	Li-mica	feldspar	fluorite	feldspar	feldspar	quartz
Analysis	22(b)	23†	24†	25	26	27	28	29(a)	30
P_2O_5	32.9	33.6	32.6	32.3	32.9	34.4	32.1	32.5	32.6
SiO_2	0.24	0.72	0.31	0.17	0.26	0.18	1.17	0.20	0.63
ThO_2	0.26	0.84	0.50	0.24	—	0.37	6.01	0.77	1.17
UO_2	0.98	2.20	0.88	0.76	0.32	0.54	0.30	0.15	0.10
Y_2O_3	32.7	39.6	30.7	29.0	30.4	39.9	36.8	28.2	26.8
Ce_2O_3	0.05	0.16	0.03	0.03	—	—	0.09	0.03	0.03
Pr_2O_3	—	0.05	0.05	0.03	0.03	0.04	0.09	0.08	0.07
Nd_2O_3	0.31	0.64	0.18	0.22	0.19	0.32	0.44	0.16	0.15
Sm_2O_3	0.23	0.89	0.34	0.17	0.22	0.61	0.80	0.49	0.41
Gd_2O_3	4.02	3.61	4.44	3.94	5.43	5.53	4.57	3.64	3.60
Tb_2O_3	0.91	0.79	1.04	1.05	1.05	0.99	0.92	1.07	1.02
Dy_2O_3	6.86	4.76	7.90	7.68	8.61	6.62	5.69	6.70	6.31
Ho_2O_3	1.50	0.98	1.87	1.80	2.00	1.32	1.23	1.28	1.33
Er_2O_3	6.70	3.88	6.92	7.30	7.23	4.26	4.38	6.50	6.39
Tm_2O_3‡	1.21	0.68	1.24	1.39	1.13	0.55	0.65	1.53	1.53
Yb_2O_3	9.43	5.15	9.56	11.2	7.82	3.07	4.20	13.9	14.0
Lu_2O_3	1.39	0.68	1.29	1.66	1.30	0.44	0.57	2.09	2.13
CaO	0.10	0.12	0.07	0.10	0.08	0.22	0.47	0.04	0.12
PbO	—	0.09	0.04	0.02	—	—	0.08	—	0.02
Total	99.8	99.4	99.9	99.1	99.0	99.4	100.6	99.3	98.9
Mole fractions									
$(Th,U,Pb)SiO_4$	0.009	0.029	0.011	0.006	0.003	0.006	0.041	0.007	0.011
$(Ca,U,Th)(PO_4)_2$	0.006		0.006	0.010		0.009	0.015	0.015	
$(La\text{-}Sm)PO_4$	0.007	0.014	0.008	0.006	0.006	0.012	0.017	0.010	0.008
$(Gd\text{-}Lu)PO_4$	0.359	0.230	0.389	0.414	0.394	0.249	0.246	0.421	0.413
YPO_4	0.618	0.725	0.587	0.564	0.582	0.725	0.681	0.548	0.538

mass spectrometry as described in Förster (1998a). The major elements were analyzed by wavelength-dispersive X-ray fluorescence spectrometry.

RESULTS

Petrographic description of xenotime and associations of primary REE-Y-Th-U-rich minerals

In the I,S-type biotite granites, xenotime is accompanied by zircon, monazite, thorite, and uranothorite and, especially in the more evolved intrusions and aplites, by Th-rich uraninite, rare cheralite-(Ce) and huttonitic monazite-(Ce). Xenotime is virtually absent in the least-evolved biotite granites, which contain allanite-(Ce) instead of monazite.

The accessory parageneses in the two-mica and S-type Li-mica granites, where xenotime is present throughout the entire series, include zircon, monazite, and Th-poor uraninite as well as cheralite-(Ce). Brabantite is observed in some evolved S-type granites (Förster 1998a).

The A-type Li-mica granites are characterized by complex accessory mineral associations, which differ for the individual plutons and typically include a wide variety of phases of primary (magmatic) and secondary origins. The accessory minerals were described in detail from the Cinovec (Zinnwald) granite (Johan and Johan 1993, 1994a, 1994b). Samples in this study contain xenotime associated with the following REE-Y-Th-U-rich accessories: zircon, monazite, solid solutions of thorite-coffinite, thorite-xenotime and thorite-zircon, yttrofluorite, pyrochlore, and diverse REE-fluorocarbonates, -oxyfluorides and -arsenates. The accessory mineral assemblage in the A-type biotite granites is less complex and comprises monazite, zircon, and thorite.

Xenotime occurs rarely as euhedral, solitary crystals with grain sizes >100 μm. Typically, xenotime is subhedral to anhedral and much smaller (10–40 μm across), and tends to be intergrown with other accessory minerals. Xenotime occurs most commonly along the margins of zircon grains, whereas intergrowths with monazite and rutile are subordinate. Xenotime was also identified as tiny exsolved (?) grains within Y-HREE-rich zircon. However, the grains are too small for analysis with the electron microprobe. In some cases, xenotime grains contain 1–2 μm size inclusions that probably are uraninite or uranothorite and are tentatively interpreted as a product of exsolution from their host. Compositionally homogeneous xenotime grains largely predominate over zoned grains. Compositional heterogeneity within single crystals constitute either core-rim zonation (commonly non-systematic and non-concentric) or irregular domains distributed within the grains.

Compared to zircon and monazite, xenotime is included more commonly within trioctahedral micas. As shown in Table 2, xenotime is also hosted in the other major minerals and, for the A-type Li-mica granites, within fluorite for which textural evidence suggests a late-magmatic origin.

Chemical compositions

Table 2 presents chemical compositions of xenotime grains determined by electron microprobe analysis, listed

TABLE 2—*Continued*

A-type Li-mica granites			A-type biotite granites	
SSH 1168-FS quartz 31(a)	ZNW 1161-FS quartz 32	ZNW 1157-FS feldspar 33	GOT Gb-71 biotite 34†	GOT Gb-71 biotite 35†
32.1	32.0	31.8	32.0	34.2
0.29	0.18	0.74	1.53	0.29
0.54	1.26	0.84	2.85	0.37
0.13	0.49	0.25	3.92	1.01
27.0	26.8	26.8	36.6	41.8
0.02	0.41	0.06	0.33	0.02
0.07	0.28	0.04	0.11	0.02
0.43	1.53	0.16	1.00	0.25
0.25	1.98	0.24	1.26	0.46
5.48	4.94	2.71	3.60	3.02
0.74	1.28	0.61	0.70	0.78
7.75	7.62	5.61	4.84	4.64
1.56	1.54	1.30	1.03	0.98
6.85	6.04	7.37	3.13	4.09
1.48	1.16	1.69	0.57	0.69
12.8	9.59	15.1	4.39	5.08
1.59	1.42	2.27	0.56	0.72
0.21	0.31	0.17	0.17	0.08
0.03	0.03	—	0.18	0.02
99.3	99.0	98.4	98.8	98.6
0.011	0.007	0.009	0.054	0.010
	0.024		0.015	0.004
0.010	0.055	0.007	0.034	0.009
0.442	0.390	0.431	0.210	0.216
0.528	0.525	0.528	0.686	0.761

according to host granite type: biotite granite, two-mica granite, S-type Li-mica granite, A-type Li-mica granite, and A-type biotite granite. Specific samples are listed that document the compositional variability within the five groups of granites. No distinctions have been made between xenotime from the Li-mica and the biotite-bearing A-type granites in the chemical variation diagrams (e.g., Figs. 2–6).

LREE. Concentrations of La, Ce, and Pr are typically low compared to the other REE in xenotime. Within a single grain, each of these three LREE may occur in concentrations near or below the detection limit of the electron microprobe (Table 2, analyses 3 and 4). A xenotime grain in quartz from the Zinnwald granite (Table 2, analysis 32) has the highest concentrations of La, Ce, and Pr (0.74 wt% combined oxides).

Concentrations of Nd and Sm range from 0.07 to 1.53 wt% Nd_2O_3 and 0.04 to 1.98 wt% Sm_2O_3 (Table 2), although in most grains the ranges are restricted to about 0.1–0.6 wt% Nd and 0.2–0.7 wt% Sm (see Fig. 2a). The xenotime grain (Table 2, analysis 32) whose neodymium and samarium concentrations plot in the upper right corner of Figure 2a has a total LREE content equivalent to 5.5 mol% (La-Sm)PO_4. Most of the xenotime grains have Sm/Nd ratios between 2 and 0.5 (Fig. 2a), although xenotime grains displaying higher (Table 2, analyses 2, 30, 31) and lower ratios (Table 2, analyses 10 and 16) also occur.

Y and HREE. The proportion of YPO_4, the main component in xenotime, ranges from 52.5 to 83.4 mol% (Fig. 3). Concentrations of Y are highest in xenotime grains from fractionated biotite granites, and lowest in xenotime grains from the A-type Li-mica granites. Xenotime from two-mica and S-type Li-mica granites is restricted in yttrium concentration (from 70 to 80 mol% YPO_4).

The HREE-PO_4 component ranges from 15.5 to 45.2 mol% (Fig. 3). The concentration ranges for the individual HREE oxides are as follows (in weight percent): Gd = 2.0–5.5, Tb = 0.4–1.3, Dy = 3.2–8.6, Ho = 0.6–2.0, Er = 2.0–7.4, Yb = 0.7–15.1, Lu = 0.1–2.3 (see Figs. 2b–2d). The Y_2O_3 content ranges from 26.8 to 46.7 wt% and correlates inversely with the HREE content (Fig. 3). Xenotime grains with the lowest concentrations of HREE are found in biotite granites, whereas xenotime grains with the highest concentrations of HREE occur in the A-type Li-mica granites.

U and Th. Both of the actinide elements, U and Th, range in concentration from below the limit of detection to several weight percent (maximum UO_2 = 6.7, maximum ThO_2 = 6.0). In most cases, xenotime incorporates greater concentrations of U than Th, especially for samples from the two-mica and S-type Li-mica granites, which have Th/U < 0.5 (Fig. 4a). The Li-mica-bearing A-type granites host xenotime grains that may have Th/U > 2 and as high as ≈10 (Table 2, analysis 28).

Substitution mechanisms for the incorporation of the actinides

The main mechanisms for the replacement of Y and REE by U and Th are charge-balancing coupled substitutions involving Si and Ca as illustrated by a plot of (Th+U+Si) vs. (P+Y+REE) (Fig. 4b). One group of analyses clusters on or near the vector (Th,U)$SiREE_{-1}P_{-1}$, reflecting solid solution between xenotime and thorite-coffinite, which have the closely packed zircon structure (Fuchs and Gebert 1958; Ni et al. 1995).

This solid solution corresponds to the cationic substitution:

$$(REE,Y)^{3+} + P^{5+} \leftrightarrow (Th,U)^{4+} + Si^{4+}. \quad (1)$$

In xenotime from the Erzgebirge granites, increased concentrations of SiO_2 are found in those grains that are rich in both ThO_2 and (ThO_2 + UO_2) (Table 2, analyses 1, 7, 9, 12, 14, 28).

On Figure 4b, many of the data points for xenotime grains are shifted toward the vector (U,Th)$CaREE_{-2}$ representing the substitution:

$$2\ (REE,Y)^{3+} \leftrightarrow (U,Th)^{4+} + Ca^{2+}. \quad (2)$$

This cationic exchange is particularly significant in xenotime from the S-type Li-mica granites but occurs also in xenotime from the other types of granites. Thus xenotime may also contain brabantite, $CaTh(PO_4)_2$, and its uranium equivalent, $CaU(PO_4)_2$, both of which are end-members of the monoclinic monazite group.

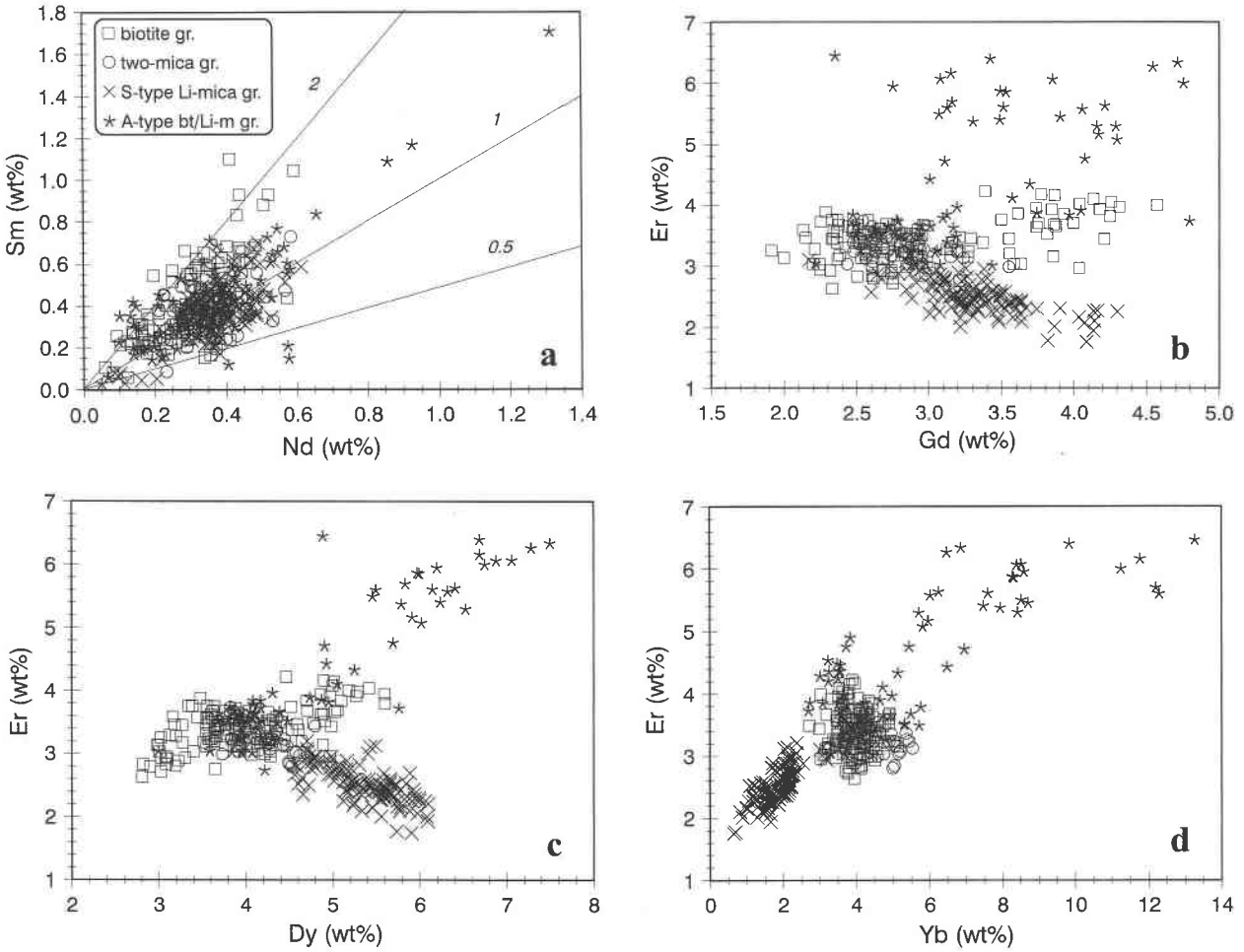

FIGURE 2. Compositional variations (in weight percent element) of REE in xenotime from the different groups of peraluminous granites. Symbols are as follows: open squares = biotite granites, open circles = two-mica granites, crosses = S-type Li-mica granites, stars = A-type biotite (bt) and Li-mica (Li-m) granites. **(a)** Sm vs. Nd. **(b)** Er vs. Gd. **(c)** Er vs. Dy. **(d)** Er vs. Yb.

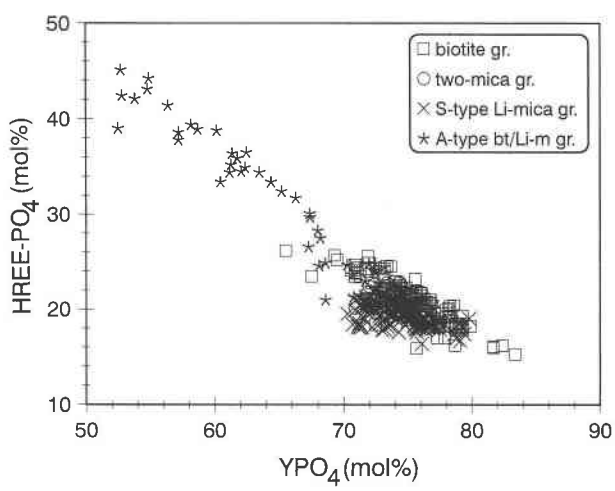

FIGURE 3. Xenotime compositions in terms of mole percent HREE-PO_4 vs. YPO_4.

Relations between xenotime and host rock composition

The stability and abundance of accessory minerals in silicate melts depends on numerous chemical and physical properties of the melt such as the activities of SiO_2, CaO, P_2O_5, and the halogens F and Cl, the oxygen fugacity, the peraluminosity, and the ratios and contents of the incorporated trace elements (Cuney and Friedrich 1987; Casillas et al. 1995). The composition of xenotime in relation to the bulk-rock concentrations of the lanthanides and actinides (e.g., Table 1), and the relative proportions among them, are explored in this section.

There appears to be no correlation between the LREE and HREE concentrations (Fig. 5a) in xenotime and the granite host. There is a greater tendency for the HREE-rich, F-rich, and P-poor Li-mica granites to contain xenotime rich in HREE than for granites of the other groups. However, a broad range of values exists for each granite type, and these ranges overlap among the different groups of granites. The LREE and HREE concentrations in xenotime remained virtually constant during magmatic dif-

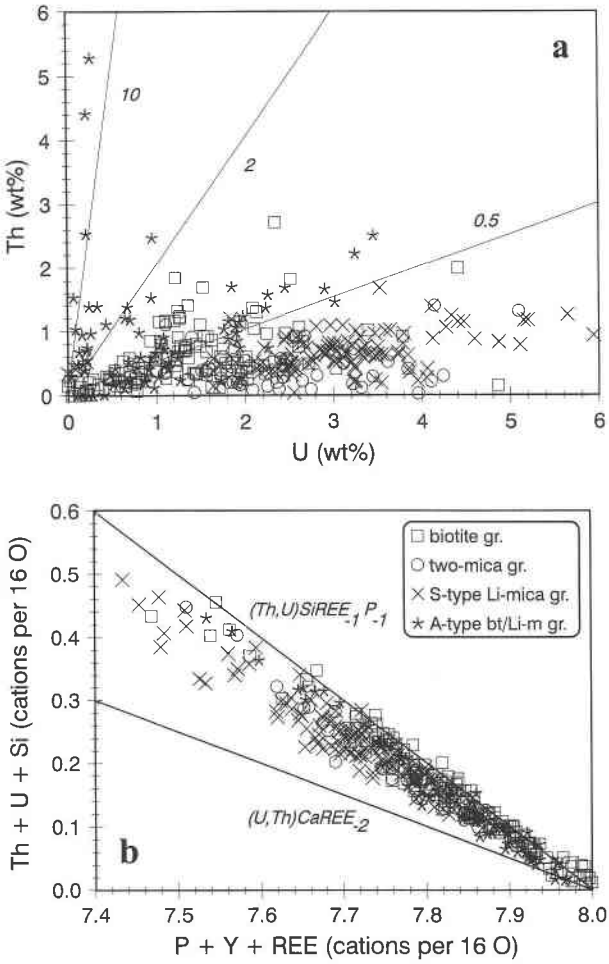

FIGURE 4. Distribution of U and Th in xenotime. **(a)** Th vs. U (in weight percent element). **(b)** Formula proportions (Th + U + Si) vs. (REE + Y + P) calculated on the basis of 16 O atoms.

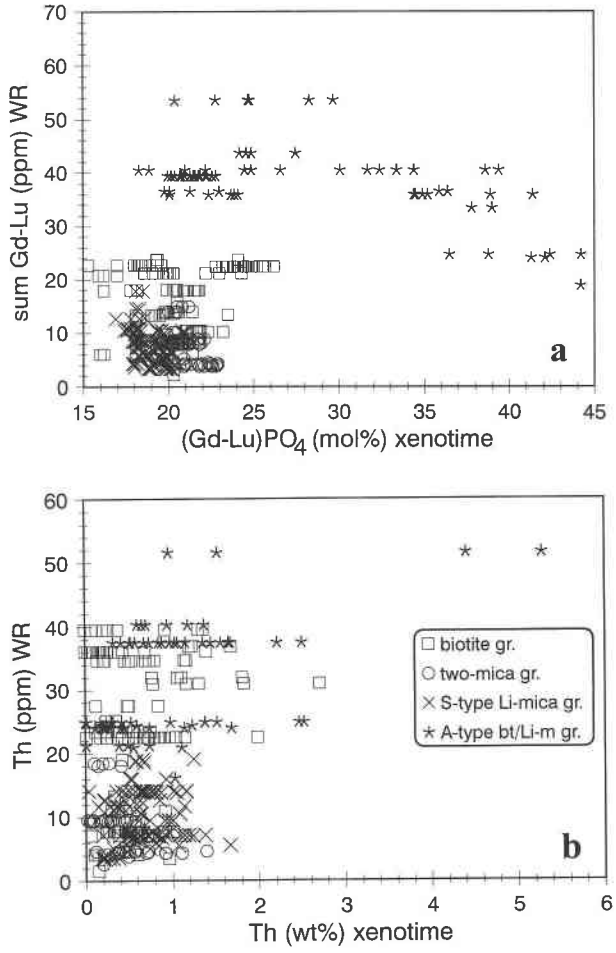

FIGURE 5. Relations between the concentrations of HREE **(a)** and Th **(b)** in whole rocks (WR) and xenotime.

ferentiation of the two-mica and S-type Li-mica granites, which involves combined monazite-xenotime-zircon-(apatite) fractionation, presumably causing a decrease in the LREE and HREE concentrations of residual melts. In contrast, more-differentiated, HREE-depleted intrusions of the A-type Li-mica granite group typically contain xenotime richest in HREE.

The distribution of Th between xenotime and host granites is similar to that of the HREE (Fig. 5b). Granites that have thorium concentrations exceeding 20 ppm (e.g., the A-type and most of the biotite granites) tend to contain xenotime that is atypically enriched in Th. Nevertheless, even these Th-rich granites typically contain xenotime with the same range of thorium concentrations as those from the two-mica and S-type Li-mica granites. The most fractionated members of these are extremely depleted in Th due to early monazite fractionation (e.g., Table 1).

Whole-rock U concentrations between 20–40 ppm are characteristic of unaltered samples of Erzgebirge granites (Förster 1998b). Even though such U contents are atypically high for granites, xenotime is not more strongly enriched in U than those from U-poor granites. The Sweetwater Wash S-type two-mica granite is U-poor (<2 ppm U) but contains xenotime with up to 6 wt% U (Wark and Miller 1993).

A weak correlation exists between the Th/U ratios of xenotime grains and their host granite. The high Th/U (~1–4) ratios in granites of A-type affinity correlate with xenotime grains that have the strongest enrichment of Th over U, whereas the low Th/U (~0.1–1) S-type Li-mica granites typically host xenotime grains in which U predominates over Th (e.g., Fig. 4a).

Although no strong correlations exist between the total concentrations of HREE in granite whole-rocks and xenotime, the relative proportions of the "lighter" group, Gd-Ho, and the "heavier" group, Er-Lu, differ significantly and distinguish among the granite types (Fig. 6a). In xenotime from the S-type Li-mica granites, the Gd-Ho/Er-Lu molar ratio approaches 5. In contrast, xenotime from the A-type Li-mica granites has ratios as low as 0.5.

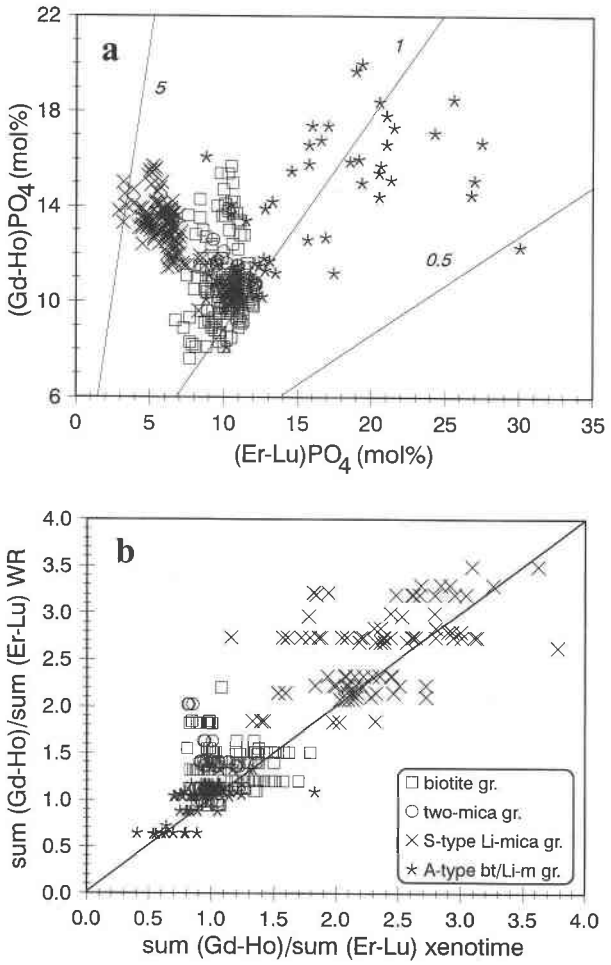

FIGURE 6. Compositional relations between the groups of "lighter" and "heavier" HREE in xenotime and granite hosts (WR). **(a)** (Gd-Ho)PO_4 vs. (Er-Lu)PO_4 (in mol%) in xenotime. **(b)** ratios of (Gd-Ho)/(Er-Lu) in whole-rock vs. xenotime.

As shown in Figure 6b, the proportions of Gd-Ho and Er-Lu in bulk rock and in xenotime are similar in many cases, irrespective of the type of host granite.

The chondrite-normalized HREE patterns of xenotime are commonly similar in shape to those of their granite hosts (e.g., compare Figs. 7a and 7e for biotite granites, Figs. 7b and 7f for two-mica granites, Figs. 7c and 7g for S-type Li-mica granites, Figs. 7d and 7h for A-type Li-mica granites). The concentrations of La, Ce, and Pr in xenotime are consistently low and close to the detection limits of the electron microprobe. This implies that observed irregularities in the LREE patterns may result from high uncertainties for these low concentrations.

The HREE patterns of some of the xenotime grains and their host rocks are distinguished by local minima at Ho and less commonly at Gd and Lu. The two elements Y and Ho can be considered a geochemical pair because of their similar ionic size and same charge (e.g., Bau 1996); however, they can be decoupled in xenotime. The ratio Y/Ho in xenotime ranges from 15 (in some of the A-type Li-mica granites) to 40 (in the evolved S-type granites), and typically corresponds to Y/Ho of the host granite. The most fractionated Y/Ho ratios observed in xenotime from this study reach 60, compared to a chondritic ratio of 28.

DISSCUSSION

Overall compositional variability of xenotime

The maximum and minimum concentrations for U, Th, Y, and the REE in xenotime from this study are close to or, in most cases, greater than those previously noted. Substantial enrichment of Sm, approaching the highest concentration from this study, was also observed in xenotime from metapelites from NE Bavaria, Germany (Franz et al. 1996), which also contain xenotime extraordinarily rich in Gd [7.9 wt% Gd_2O_3 (published value recalculated by the author for interference of Ho$L\alpha_1$ on Gd$L\beta_1$)]. Xenotime with concentrations of Gd lower than those from this study have been reported in granitic rocks and migmatites (Casillas et al. 1995; Bea 1996a), and especially granitic pegmatites (0.5 wt% at a minimum; Demartin et al. 1991; Petersen and Gault 1993). The highest concentrations of Dy determined in this study are approached by those in xenotime from some orthogneisses in Canada (8.3 wt% Dy_2O_3; Pan 1997). A xenotime grain distinctly higher in Y concentration (53.5 wt% Y_2O_3, corresponding to 90.7 mol% YPO_4) was described from an Alpine granite pegmatite (Demartin et al. 1991). Finally, the maximum concentrations of Th and U in xenotime from the Erzgebirge granites are similar to those in xenotime from aplites within the Sweetwater Wash two-mica granitic pluton (e.g., Fig. 6 in Wark and Miller 1993).

The combination of compositional data from the literature and from this study yield the following ranges of concentrations (measured by EPMA) for Y, REE, U, and Th in xenotime of known origin and approximately stoichiometric composition (in weight percent): Y_2O_3 = 26.8–53.5, Nd_2O_3 = <0.02–1.5, Sm_2O_3 = <0.02–2.0, Gd_2O_3 = 0.5–7.9, Tb_2O_3 = 0.3–1.3, Dy_2O_3 = 2.1–8.6, Ho_2O_3 = 0.5–2.0, Er_2O_3 = 1.9–7.4, Yb_2O_3 = 0.7–15.1, Lu_2O_3 = 0.1–2.3; UO_2 = <0.01–6.7, ThO_2 = <0.01–6.0.

Uranium and thorium substitutions

Typically, the U/Th ratio in xenotime from the Erzgebirge granites exceeds 1. This finding corroborates previous observations (Wark and Miller 1993; Franz et al. 1996; van Emden et al. 1997) that xenotime, unlike monazite (e.g., Förster 1998a), exhibits a substantial preference of U over Th. However, the U/Th ratio in xenotime is highly variable and there are some grains in the A-type, Li-mica granites in which U/Th ≤ 0.1.

In principle, this study confirms the results of van Emden et al. (1997) that the incorporation of U and Th in xenotime is controlled mainly by substitution [1] (see Fig. 4b). This coupled substitution has been shown by Franz et al. (1996) to be the main mechanism for the incorporation of the actinides in xenotime from metapelites. The

generally prominent role of the substitution reaction [1] can be explained by the size restraints imposed by the zircon structure-type of xenotime. This structure accommodates Si^{4+} but precludes significant amounts of other appropriate charge-balancing cations such as Ca^{2+} because of its larger size in comparison to the HREE:

As a result, substitution [2] should be of minor importance. However, in xenotime from granite, it may be as important as (e.g., Table 2, analyses 1, 5, 18, 19) or even more important (e.g., Table 2, analyses 10, 15, 16, 28, 32) than substitution [1] in which Si^{4+} is the counterbalancing ion. Unlike monazite, in xenotime the coupled substitution of Ca+U is presumably favored over Ca+Th (van Emden et al. 1997). This is attributed to differences in the average effective ionic radius ($\bar{r}$) for Ca^{2+} (1.12 Å) and U^{4+} (1.00 Å), which is close to the radius of the HREE Gd^{3+} (1.053 Å) whereas the average radius for Ca^{2+} and Th^{4+} (1.05 Å) is closer to that of the LREE Sm^{3+}(1.079 Å), for cations in eightfold coordination (ionic radii from Shannon 1976). In about 70% of the xenotime grains of this study, substitutions involving Si and Ca occur together (see Fig. 4b).

Within the four groups of granites discussed herein, substitutions [1] and [2] are equally important in monazite-group minerals (Förster and Tischendorf 1994; Förster 1998a). Substitution [1], which leads toward the end-member huttonite ($ThSiO_4$) and its U equivalent, typically dominates the incorporation of actinides into monazite from biotite granites and A-type biotite and Li-mica granites; xenotime is abundant in these rocks and rich in the coffinite and thorite end-members (see Fig. 4b). In contrast, the accomodation of Th and U in monazite from the two-mica and S-type Li-mica granites results mainly from substitution [2], which also plays a significant role in the associated xenotime.

Conditions of mineral formation

In principle, accessory minerals in granite such as monazite, zircon, thorite, and apatite may form as primary (magmatic) or secondary (metasomatic) phases. They may be early to late, in equilibrium or in disequilibrium, or they may represent fragments of restite. This holds true also for the xenotime grains studied herein, making all the observed compositional variations difficult to explain.

Most xenotime grains were dated by the chemical U-Th-total Pb method as described by Suzuki and Adachi (1991) and Rhede et al. (1996b). Within the accuracy of the method (±30–50 Ma), these grains are chronologically homogeneous and of Variscan age (350–250 Ma), corresponding to the emplacement ages of their host granites as measured independently by U-Pb monazite and K-Ar biotite isotopic dating (325–290 Ma; e.g., Förster et al. 1998). Thus, the dated xenotime grains were apparently not inherited from older source rocks.

As previously shown, the HREE-Th-rich A-type Li-mica granites are more likely to host xenotime abnormally enriched in these elements than are the HREE-Th-poor S-type Li-mica granites. However, the concentrations of the lanthanides and actinides show a broad range of values that overlap among the five major groups of granites, and among differently fractionated samples in multi-stage plutons. For example, xenotime in the Erzgebirge granites does not display a systematic increase in the concentrations of Th and U from granites to more differentiated aplites, as described for the Sweetwater Wash pluton by Wark and Miller (1993). Unlike monazite (e.g., Förster 1998a), xenotime does not record well the differences and systematic changes in the contents of U and Th that occurred during magma fractionation in the various types of granitic melts. The same holds true for variations in the total LREE concentrations.

As predicted by Wark and Miller (1993), xenotime should reflect the spatial and temporal effects of crystallization within a closed system (in-situ fractionation), and hence might be expected to show compositional variations on a thin-section scale. Although xenotime from the Erzgebirge granites exhibits such variability (e.g., Figs. 5a and 5b), specific compositions of grains cannot be correlated with a particular mineral host or associated accessory mineral, or with a specific crystal texture and habit. However, as already noted by Wark and Miller (1993), the paragenesis in equigranular granites (of which most of the Erzgebirge xenotime-bearing granites are examples) is not easy to determine. Moreover, important xenotime-hosting silicates such as quartz, feldspars, and trioctahedral micas may persist over essentially the entire crystallization interval. These facts complicate interpretations of in-situ fractionation. Another mechanism that might explain the compositional heterogeneity of xenotime on the thin-section scale is REE-phosphate supersaturation, perhaps accompanying the breakdown of previous REE-bearing phases. Xenotime grains of different compositions could form simultaneously in such circumstances and persist together either stably or metastably in response to gradients in the activity of selected species in the melt or fluid.

Monotonic chemical zoning within individual grains should also record the process of in-situ fractionation (e.g., Wark and Miller 1993). However, zoning in xenotime in the Erzgebirge granites is typically complex and non-systematic. As suggested by Wark and Miller (1993), chemical zoning likely reflects local spatial and short-term diffusion-controlled temporal changes in melt composition that occurred adjacent to growing major minerals and the growing accessory crystal itself.

The timing of xenotime formation with respect to magmatic evolution can be determined for those grains having discontinuous HREE patterns, e.g., downward kinks at Gd, Lu, and more commonly Ho, and fractionated Y/Ho ratios. These xenotime grains typically are accompanied by other accessory minerals that also show uncommon compositions. Depending on the type of host granite, these include: (1) Th-U-rich monazite-(Ce), cheralite-(Ce), and brabantite displaying local minima at La and Nd in their LREE patterns (Förster 1998a); (2) Y- and

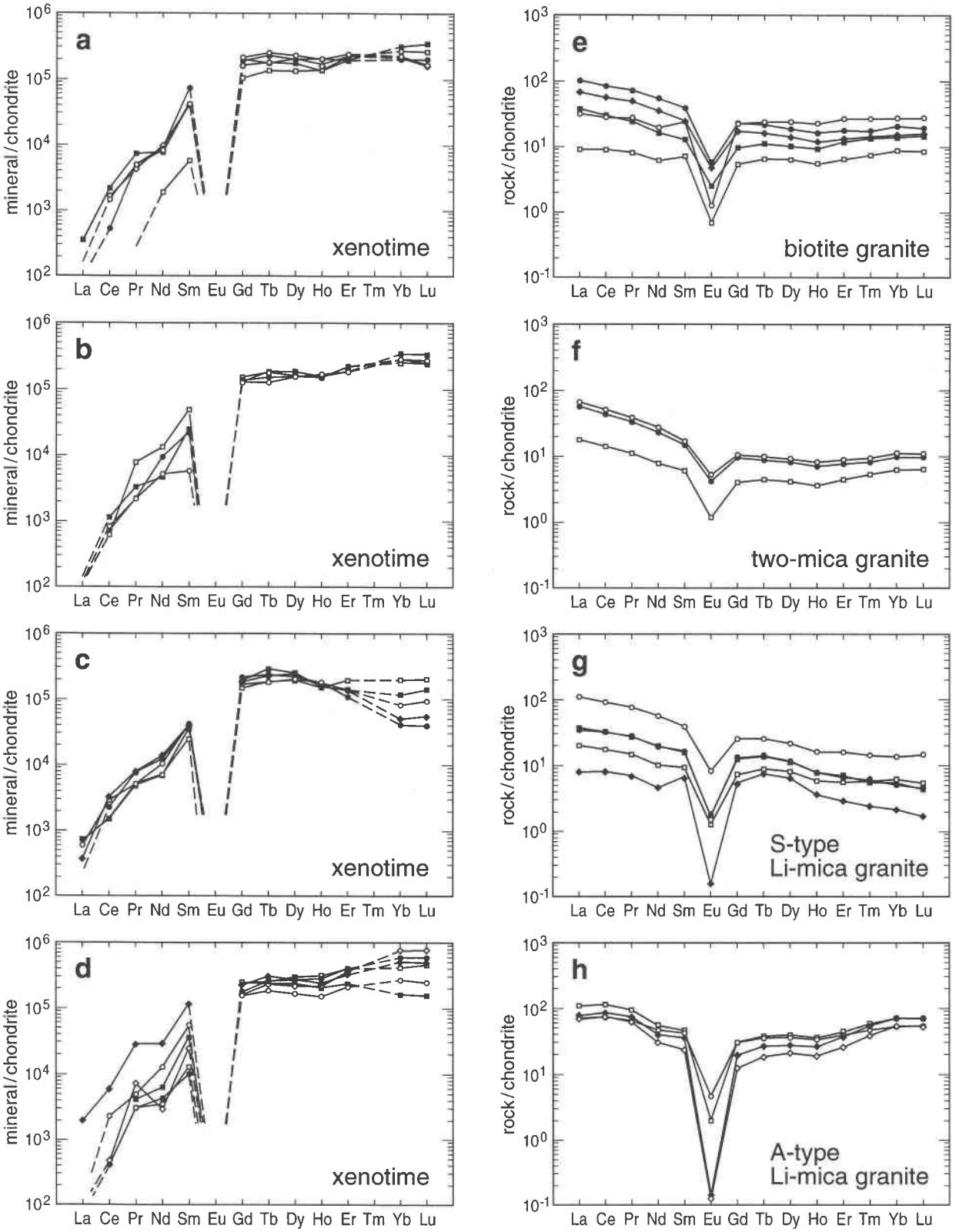
a
xenotime
b
xenotime
c
xenotime
d
xenotime
e
biotite granite
f
two-mica granite
g
S-type
Li-mica granite
h
A-type
Li-mica granite
mineral/chondrite
rock/chondrite
La Ce Pr Nd Sm Eu Gd Tb Dy Ho Er Tm Yb Lu

Zr-rich, F-bearing and hydrated metamict thorite showing fractionated Y/Ho (45–5) and Zr/Hf ratios (50–3); and (3) F-bearing and hydrated, metamict zircon possessing low and non-chondritic Zr/Hf ratios (down to 4). The combination of, and apparent link between, non-chondritic Y/Ho and Zr/Hf ratios with discontinuous REE patterns, which are commonly referred to as the lanthanide tetrad effect (e.g., Masuda and Agaki 1989), occur in granite samples from highly evolved silicic magmatic systems (Bau 1997). These data suggest that xenotime with fractionated Y/Ho ratios, together with their preferential occurrence in the more evolved intrusions within each of the five major groups of Erzgebirge granites, were formed either by crystallization from fluid-rich residual melts or from supercritical fluids. Thus these xenotime crystals record information from the very latest stages of crystallization and associated deuteric alteration.

In the A-type Li-mica granites, formation of the uncommonly HREE-rich xenotime with low Y/Ho and Gd-Ho/Er-Lu ratios also may have occurred by breakdown of zircon (Dy/Yb < 0.2) or thorite (Dy/Yb = 0.2–1.3), or both, which commonly show a preference for the elements of the Er-Lu group. Furthermore, metasomatic reaction of xenotime grains with volatile-rich residual silicate liquids or supercritical solutions may have released some HREE, which could reprecipate to form the HREE-rich rims or domains. Altered HREE-rich xenotime itself shows the same shape of HREE patterns and similarly low Y/Ho ratios but contains some fluorine (up to 1.2 wt%). Oxide sums around 95 wt% suggest that it is also hydrated.

Implications

Xenotime has been shown to be an accessory mineral whose chemical composition varies considerably with respect to both the total concentrations of lanthanides and actinides and their relative proportions. It is dominated by the end-members HREE-PO_4 and YPO_4, which constitute more than 90 mol% of the mineral. Over 90% of the grains analyzed in this work contain 70–80 mol% YPO_4, and 16–25 mol% HREE-PO_4. The full data set, however, supports complete miscibility between the theoretical end-members HREE-PO_4 and YPO_4 in the range 16–45 mol% HREE-PO_4.

Substitutions of coffinite-thorite $(U,Th,Pb)SiO_4$ and brabantite $(Th,U,Ca)(PO_4)_2$ are low (mostly <2 mol%, but range up to 6.1 and 5.9 mol%, respectively). Xenotime can incorporate a monazite (La-Sm)PO_4 component at similar levels (up to 5.5 mol%). The highest total fraction of coffinite-thorite, brabantite, and monazite substitutions in a single grain is 10.9 mol%.

On the basis of cation sizes, substitution [1] is considered to be the main mechanism for incorporating U and Th into xenotime (van Emden et al. 1997). However for several xenotime grains reported here, it is in fact substitution [2] that accounts for most of the U and Th. This implies that factors such as the availability of the charge-balancing cations Si^{4+} and Ca^{2+} may be more significant in controlling the mechanism of incorporation of the actinides than are cation-radius limitations imposed by the xenotime structure (e.g., van Emden et al. 1997).

Xenotime constitutes an accessory mineral in which decoupling of Y and the HREE can occur. Thus, xenotime from highly evolved, late-stage granites is commonly characterized by non-chondritic Y/Ho ratios. The Y/Ho ratio may evolve in both directions, i.e., xenotime may show either higher (such as those occurring in the S-type Li-mica granites) or lower (in the A-type Li-mica granites) ratios than C1-chondrites. Xenotime with fractionated Y/Ho ratios and HREE patterns suggestive of the lanthanide tetrad effect records information from the latest stages of residual melt crystallization and some associated high-temperature alteration, where processes such as chemical complexation become increasingly more important (e.g., Bau 1996).

The close similarities between xenotime and host granites with respect to their HREE patterns (e.g., Fig. 7) highlight the importance of this mineral as a carrier of the HREE. Based on this observation, one might predict what the HREE pattern of the host granite would look like from the HREE patterns of the xenotime, or vice versa. However, identical correspondence between the HREE patterns of xenotime and bulk rock is not expected because other accessory minerals such as monazite (which preferentially concentrates the LREE and Gd, Tb, and Dy), zircon (Yb and Lu), thorite and apatite should also contribute to the measured bulk-rock concentrations of the HREE. Nonetheless, this prediction is substantiated by mass-balance calculations for a moderately evolved two-mica granite and a highly evolved F-poor biotite granite from the Erzgebirge. In these granites, xenotime accounts for ~30–40% of the whole-rock Gd contents, but ~60–75% of the Yb contents.

Correlations of the distribution of the actinides, Th and

←

Figure 7. Comparison of chondrite-normalized REE patterns of xenotime (**a–d**) and host granites (**e–g**). Within each of the four pairs of diagrams (a–e, b–d, c–f, d–g), xenotime and host rock are identified by identical symbols. (See Table 2 for the number of the xenotime analysis; also, see below). The symbols are as follows: **(a)** open circles = analysis 1, dots = analysis 2, open squares = analysis 4, filled squares = analysis 6, open diamonds = analysis 7. **(b)** open circles = analysis 10, dots = analysis 11, open squares = analysis 12, filled squares = analysis 13. **(c)** open circles = analysis 14, dots = analysis 17, open squares = analysis 18, filled squares = analysis 20, filled diamonds = analysis 21. **(d)** open circles = analysis 23, dots = analysis 25, open squares = analysis 26, filled squares = analysis 27, open diamonds = analysis 30, filled diamonds = analysis 32. Chondrite data are from Anders and Grevesse (1989).

U, between xenotime and whole-rocks are weak or nonexistent. This suggests that other minerals (e.g., zircon, monazite, thorite, and uraninite) are also significant hosts of these elements. Indeed, mass-balance calculations for the Erzgebirge granites studied herein show that ~80–90% of the whole-rock Th content may be attributed to monazite plus thorite, whereas in most granites uraninite is the main repository of U (40–90% of the whole-rock budget). Granites lacking thorite and uraninite are the potential hosts of xenotime strongly enriched in Th and U, respectively.

Attempts to model the HREE and Y evolution of composite granitic plutons either qualitatively or quantitatively requires careful consideration of the role of xenotime as the major host for these elements, as well as its potential diversity in the concentrations of the lanthanides and actinides. However, even if relevant information on the composition of xenotime were available, the process and timing of xenotime formation is only poorly known, which is also the case for other accessory minerals in granites. Thus, petrogenetic modeling that makes use of the REE, U, and Th in granitic rocks, should be done with caution and with consideration of accessory minerals like xenotime and monazite (e.g., Bea 1996a).

Acknowledgments

The author is indebted to D. Rhede and O. Appelt for their help with the electron microprobe work. G. Tischendorf is thanked for his assistance in collecting the whole-rock samples. Sampling of some of the granite occurrences in the eastern Erzgebirge and their bulk-rock chemical analyses was done in close collaboration with R. Seltmann. XRF and ICP-MS whole-rock analyses have been performed by R. Naumann and P. Dulski. The paper benefited from valuable comments of Brad Jolliff, Michael Wolf and an anonymous reviewer. Finally, I wish to acknowledge the assistance of Bob Trumbull and Dan Harlov for improving a first draft of this manuscript.

References cited

Åmli, R. (1975) Mineralogy and rare earth geochemistry of apatite and xenotime from the Gloserheia granite pegmatite, Froland, southern Norway. American Mineralogist, 60, 607–620.

Anders, E. and Grevesse, N. (1989) Abundances of the elements: meteoric and solar. Geochimica et Cosmochimica Acta, 53, 197–214.

Bea, F. (1996a) Residence of REE, Y, Th and U in granites and crustal protoliths; implications for the chemistry of crustal melts. Journal of Petrology, 37, 521–552.

———(1996b) Controls on the trace element composition of crustal melts. Transactions of the Royal Society of Edinburgh: Earth Sciences, 87, 33–41.

Bea, F. and Montero, P.G. (1997) Rare earth elements, yttrium, thorium, and uranium in crustal melting—The behavior of accessories during metamorphism and anatexis of metapelites: The Kinzingite Formation (Ivrea-Verbano, northern Italy). 7th Annual V.M. Goldschmidt Conference, p. 21. LPI Contribution no. 921. The Lunar and Planetary Institute, Houston.

Bau, M. (1996) Controls on the fractionation of isovalent trace elements in magmatic and aqueous systems: evidence from Y/Ho, Zr/Hf, and lanthanide tetrad effect. Contributions to Mineralogy and Petrology, 123, 323–333.

———(1997) The lanthanide tetrad effect in highly evolved felsic igneous rocks—a reply to the comment by Y. Pan. Contributions to Mineralogy and Petrology, 128, 409–412.

Casillas, R., Nagy, G., Pantó, G., Brändle, J., and Fórizs, I. (1995) Occurrence of Th, U, Y, Zr, and REE-bearing accessory minerals in late-Variscan granitic rocks from the Sierra de Guadarrama (Spain). European Journal of Mineralogy, 7, 989–1006.

Childe, F., Doig, R. and Gariépy, C. (1993) Monazite as a metamorphic chronometer, south of the Greenville Front, western Quebec. Canadian Journal of Earth Sciences, 30, 1056–1065.

Cuney, M. and Friedrich, M. (1987) Physicochemical and crystal-chemical controls on accessory mineral paragenesis in granitoids: implications for uranium metallogenesis. Bulletin Minéralogie, 110, 235–247.

Demartin, F., Pilati, T., Diella, V., Donzelli, S., Gentile, P., and Gramaccioli, C.M. (1991) The chemical composition of xenotime from fissures and pegmatites in the Alps. Canadian Mineralogist, 29, 69–75.

Förster, H.-J. (1997) Xenotime—its compositional diversity and bearing on the HREE evolution in peraluminous granites. 7th Annual V.M. Goldschmidt Conference, p. 73–74. LPI Contribution no. 921. The Lunar and Planetary Institute, Houston.

———(1998a) The chemical composition of REE-Y-Th-U-rich accessory minerals in peraluminous granites of the Erzgebirge-Fichtelgebirge region, Germany. Part I: The monazite-(Ce)—brabantite solid solution series. American Mineralogist, 83, 259–272.

———(1998b) The chemical composition of uraninite in Variscan granites of the Engebirge, Germany. Mineralogical Magazine (in press).

Förster, H.-J. and Rhede, D. (1995) Composition of monazite and xenotime from the Fichtelgebirge granites—An electron microprobe study. Berichte der Deutschen Mineralogischen Gesellschaft, Beihefte zum European Journal of Mineralogy, 7, 68.

Förster, H.-J., Seltmann, R., and Tischendorf, G. (1995) High-fluorine, low-phosphorus A-type (post-collision) silicic magmatism in the Erzgebirge. 2nd Symposium on Permocarboniferous Igneous Rocks, Extended Abstracts. Terra Nostra, 7, 32–35.

Förster, H.-J. and Tischendorf, G. (1994) The western Erzgebirge-Vogtland granites: implications to the Hercynian magmatism in the Erzgebirge-Fichtelgebirge anticlinorium. In R. Seltmann, H. Kämpf, and P. Möller, Eds., Metallogeny of Collisional Orogens, p. 35–48. Czech Geological Survey, Prague.

Förster, H.-J., Tischendorf, G., Seltmann, R., and Gottesmann, B. (1998) Die varszischen Granite des Erzgebirges: neue Aspekte aus stoffflicher sicht. Zeitschrift für geologische Wissen-schaften (in press).

Franz, G., Andrehs, G., and Rhede, D. (1996) Crystal chemistry of monazite and xenotime from Saxothuringian-Moldanubian metapelites, NE Bavaria, Germany. European Journal of Mineralogy, 8, 1097–1118.

Fuchs, L.H. and Gebert, E. (1958) X-ray studies of synthetic coffinite, thorite, and uranothorites. American Mineralogist, 43, 243–248.

Gottesmann, B., Seltmann, R., and Förster, H.-J. (1995) Felsic subvolcanic intrusions within the Eibenstock granite pluton (Saxony, Germany): The Gottesberg volcano-plutonic system. 2nd Symposium on Permocarboniferous Igneous Rocks, Extended Abstracts. Terra Nostra, 7, 49–53.

Gratz, R. and Heinrich, W. (1997) Monazite-xenotime thermobarometry: Experimental calibration of the miscibility gap in the binary system $CePO_4$-YPO_4. American Mineralogist, 82, 772–780.

Hawkins, D.P. and Bowring, S.A. (1997) U-Pb systematics of monazite and xenotime: case studies from the Paleoproterozoic of the Grand Canyon, Arizona. Contributions to Mineralogy and Petrology, 127, 87–103.

Heinrich, W., Andrehs, G., and Franz, G. (1997) Monazite-xenotime miscibility gap thermometer. 1. An empirical calibration. Journal of Metamorphic Geology, 15, 3–16.

Hodges, K.V., Parrish, R.R., Housh, T.B., Lux, D.R., Burchfiel, D.R., Royden, L.H., and Chen, Z. (1992) Simultaneous Miocene extension and shortening in the Himalayan orogen. Science, 258, 1466–1470.

Johan, Z. and Johan, V. (1993) Accessory minerals of the Cínovec granitic cupola; Behaviour of REE in F- and CO_2-rich fluids. In F. Fenoll Hach-Ali, J. Torres-Ruiz, and F. Gervilla, Eds., Current Research in Geology Applied to Ore Deposits, p. 625–628. La Guioconda, Granada.

———(1994a) Accessory minerals of the Cínovec (Zinnwald) granite cupola, Czech Republic Part 1: Nb-, Ta-, and Ti-bearing oxides. Mineralogy and Petrology, 51, 323–343.

———(1994b) Oxyfluorures de terres rares de la cupole granitique de Cínovec (Zinnwald), République tchèque. Comptes Rendus de l'Académie des Sciences, Serie 2, 318, 1333–1340.

Kamber, B.S., Frei, R., Gibb, A.J., and O'Nions, R.K. (1996) Granulite

chronometry—how accurately can we interpret precise ages? Journal of Conference Abstracts, 1, 300.

Kerrich, R. and King, R. (1993) Hydrothermal zircon and baddeleyite in Val-d'Or Archean mesothermal gold deposits: characteristics, compositions, and fluid-inclusion properties, with implications for timing of primary gold mineralization. Canadian Journal of Earth Sciences, 30, 2334–2351.

Köppel, V. and Grönenfelder, M. (1975) Concordant U-Pb ages of monazite and xenotime from the central Alps and the timing of the high temperature Alpine metamorphism, a preliminary report. Schweizer Mineralogische und Petrographische Mitteilungen, 55, 129–132.

Masuda, A. and Agaki, T. (1989) Lanthanide tetrad effect observed in leucogranites from China. Geochemical Journal, 23, 245–253.

Miller, C.F., Hanchar, J.M., Wooden, J.L., Bennett, V.C., Harrison, T.M., Wark, D.A., and Foster, D.A. (1992) Source region of a granite batholith: evidence from lower crustal xenoliths and inherited accessory minerals. Transactions of the Royal Society of Edinburgh. Earth Sciences, 83, 49–62.

Ni, Y., Hughes, J.M., and Mariano, A.M. (1995) Crystal chemistry of the monazite and xenotime structures. American Mineralogist, 80, 21–26.

Pan, Y. (1997) Zircon- and monazite-forming metamorphic reactions at Manitouwadge, Ontario. Canadian Mineralogist, 35, 105–118.

Petersen, O.V. and Gault, R.A. (1993) Xenotime from the Narssârssuk pegmatite, south Greenland. Neues Jahrbuch für Mineralogie Monatshefte, 6, 259–264.

Pointer, C.M., Ashworth, J.R., and Ixer, R.A. (1988) The zircon-thorite mineral group in metasomatized granite, Ririwai, Nigeria 1. Geochemistry and metastable solid solution of thorite and coffinite. Mineralogy and Petrology, 38, 245–262.

Reed, S.J.B. and Buckley, A. (1998) Rare-earth element determination in minerals by electron-probe microanalysis: application of spectrum synthesis. Mineralogical Magazine, 62, 1–8.

Rhede, D., Förster, H.-J., and Teufel, S. (1996a) Th-U-Pb dating of accessory minerals by electron microprobe. Journal of Conference Abstracts, 1, 507.

Rhede, D., Wendt, I. and Förster, H.-J. (1996b) A three-dimensional method for calculating independent chemical U/Pb- and Th/Pb-ages of accessory minerals. Chemical Geology, 130, 247–253.

Roeder, P.L. (1985) Electron-microprobe analysis of minerals for rare-earth elements: use of calculated peak-overlap corrections. Canadian Mineralogist, 23, 263–271.

Sagon, J.P. and Sabourdy, G. (1993) Le xenotime, un marqueur de l'Unite inferieure des gneiss dans le centre Limousin, Massif Central, Francais. Comptes Rendus de l'Académie des Sciences, Serie 2, 317, 1461–1468.

Shannon, R.D. (1976) Revised effective ionic radii and systematic studies of interatomic distances in halides and chalcogenides. Acta Crystallographica, A32, 753–767.

Štemprok, M. and Seltmann, R. (1994) The metallogeny of the Erzgebirge (Krušné hory) In R. Seltmann, H. Kämpf, and P. Möller, Eds., Metallogeny of Collisional Orogens, p. 61–69. Czech Geological Survey, Prague.

Suzuki, K. and Adachi, M. (1991) Precambrian provenance and Silurian metamorphism of the Tsubonosawa paragneiss in the South Kitakami, terrane, Northeast Japan, revealed by the chemical Th-U-total Pb isochron ages of monazite, zircon, and xenotime. Geochemical Journal, 25, 357–376.

Thorpe, R.S., Tindle, A.G., and Gledhill, A. (1990) The petrology and origin of the Tertiary Lundy granite (Bristol Channel, UK). Journal of Petrology, 31, 1379–1406.

Tischendorf, G. and Förster, H.-J. (1994) Hercynian granite magmatism and related metallogenesis in the Erzgebirge: A status report. In K.V. Gehlen and D.D. Klemm, Eds., Mineral Deposits of the Erzgebirge/Krušné hory (Germany/Czech Republic). Monograph Series on Mineral Deposits, 31, 5–23.

van Emden, B., Thornber, M.R., Graham, J., and Lincoln, F.J. (1997) The incorporation of actinides in monazite and xenotime from placer deposits in western Australia. Canadian Mineralogist, 35, 95–104.

Ward, C.D., McArthur, J.M., and Walsh, J.N. (1992) Rare earth element behavior during evolution and alteration of the Dartmoor granite, SW England. Journal of Petrology, 33, 785–815.

Wark, D.A. and Miller, C.F. (1993) Accessory mineral behavior during differentiation of a granite suite: monazite, xenotime, and zircon in the Sweetwater Wash pluton, southeastern California, U.S.A. Chemical Geology, 110, 49–67.

Wolf, M.B. and London, D. (1995) Incongruent dissolution of REE- and Sr-rich apatite in peraluminous granitic liquids: Differential apatite, monazite, and xenotime solubilities during anatexis. American Mineralogist, 80, 765–775.

Manuscript received September 4, 1997
Manuscript accepted July 15, 1998
Paper handled by Brad L. Jolliff